

The Effect of Dopant Additions on the Microstructure of Boron Fibers Before and After Reaction to MgB₂

James V. Marzik¹, Raymond J. Suplinskas¹, William J. Croft², Warren J. MoberlyChan²,
John D. DeFouw³, and David C. Dunand³

¹Specialty Materials, Inc., Lowell, MA, U.S.A.

²Harvard University, Cambridge MA, U.S.A.

³Northwestern University, Evanston, IL, U.S.A.

ABSTRACT

Boron fibers made by a commercial chemical vapor deposition (CVD) process have been used as precursors for the formation of magnesium diboride (MgB₂) superconducting wires. Prior to a reaction with magnesium, the addition of dopants such as carbon and titanium to the boron fiber has been shown to enhance the superconducting properties of MgB₂. These dopants also influence the kinetics of the reaction with magnesium. In this study, the effect of carbon dopant additions on the microstructure of boron fibers was investigated using powder x-ray diffraction, scanning electron microscopy (SEM) and transmission electron microscopy (TEM). Additionally, bundles of boron fibers were pressure infiltrated with molten magnesium and reacted at elevated temperatures. The microstructure and microchemistry of the fiber-metal interfaces were investigated by TEM and energy dispersive x-ray analysis (EDS).

INTRODUCTION

Chemically vapor deposited (CVD) boron fibers [1] have been used for over three decades as a composite reinforcement in a number of structural aerospace applications. Of more recent interest is the use of CVD boron (B) fibers as precursors for the synthesis of MgB₂ superconductors. The discovery of superconductivity in MgB₂ at temperatures near 40K [2] has provided a technical opportunity to achieve high performance superconductors with lower fabrication and operating costs. B fibers can be converted to MgB₂ via reaction with Mg vapor [3], in principle eliminating a separate wire-forming manufacturing step. It has been shown [4-7] that doping the B starting material by co-deposition of the dopant and boron through CVD yields improved superconductor properties when the material is converted to MgB₂. Significant increases in both the critical current density, ($J_c \sim 5 \times 10^6$ A cm⁻² at 5K) and the upper critical magnetic field ($H_{c2}(0) > 32$ T) have been demonstrated. Further, CVD B fibers have been infiltrated with liquid magnesium, and subsequently reacted to continuous MgB₂ fibers resulting in Mg/MgB₂ composites after solidification of the excess metal [8]. Hence, the potential exists for a process, based on existing commercial technology, to produce continuous, optimally doped MgB₂ superconducting wires embedded within a ductile, conductive metallic matrix (Figure 1).

The introduction of carbon impurities into B fibers by CVD methods results in homogeneous dopant distribution and predictable dopant concentrations, based on the reported superconducting properties [6] of doped B fibers that were converted to Mg(B_{1-x}C)₂. However, it was observed that increases in the dopant concentration in B fibers resulted in significant decreases in the reaction rates during the formation of doped MgB₂ by the reaction with Mg vapor. This change in reaction rates motivated the work reported here, in which doped B fibers are characterized prior to and after their conversion to MgB₂.

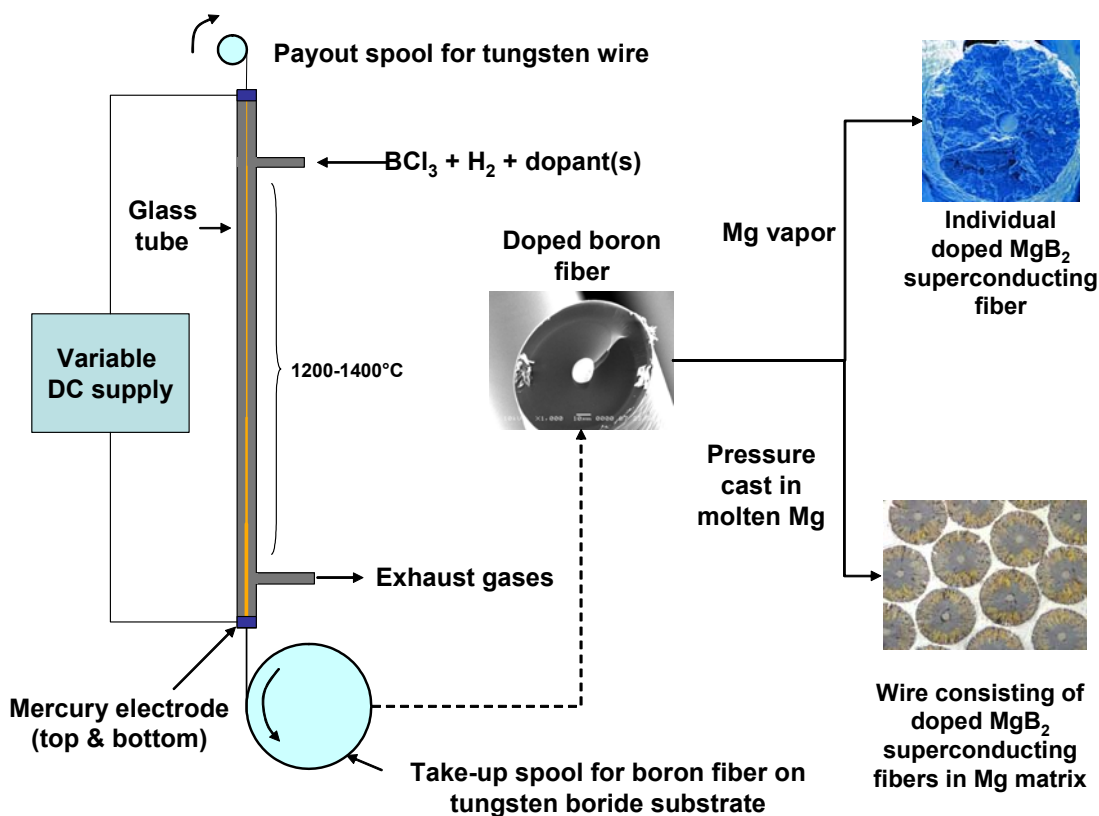


Figure 1. Process diagram showing CVD synthesis of boron fiber [1] and conversion to MgB₂ by reaction with magnesium vapor [3-7, 9] or molten Mg [8]

EXPERIMENTAL

The B fibers used here were synthesized using a modification of a commercial CVD process [1]. A 12 μ m diameter tungsten wire was drawn continuously through a 2-meter vertical glass reactor that was sealed at the top and bottom by pools of mercury. The mercury forms both an electrical contact and a gas seal. A mixture of boron trichloride (BCl₃) and hydrogen (H₂) was admitted through an inlet at the top and spent process gases were exhausted through an outlet near the bottom. The wire in the reactor is resistively heated to 1300-1400°C by application of a DC voltage to the mercury seals. At this temperature, the BCl₃ is reduced by the H₂; pure, solid, amorphous elemental boron was deposited and byproduct hydrogen chloride was exhausted. The diameter of the boron produced is controlled by the draw rate of the wire through the reactor; a rate of 3-4 m/min results in a 100 μ m B fiber (with a reacted tungsten boride core, primarily W₂B₅) being spooled continuously at the bottom. Carbon-doped B fibers were prepared similarly to undoped B fibers described above, with the addition of methane to the BCl₃ and H₂ reaction mixture. The composition (atomic %) of carbon in the gas mixture relative to boron was 0.5, 1.0, 1.4, 2.0, and 3.0%. Continuous lengths of 80 μ m diameter C-doped B fibers were produced. In this paper, the values used for dopant levels were the gas phase atomic ratios of carbon to boron. Initial analytical work indicates that the actual concentrations of carbon in the deposit may be approximately 50% higher than the gas phase concentration.

SEM/EDS analyses were carried out on a digital SEM (JEOL 5610), and a ThermoNoran System Six EDS system. TEM analyses were performed on a JEOL 2010-FEG (field emission gun) microscope operating at 200kV and a Philips EM420 operating at 100kV. EDS analyses were carried out in STEM (scanning transmission electron microscopy) mode, using an EDAX EDAM-III detector with Emispec Cynapse software. X-ray diffraction patterns were obtained using a Scintag Model XDS-2000 x-ray diffractometer calibrated with a NIST silicon standard. Copper $K\alpha$ radiation was detected with a germanium crystal cooled to 77K. The diffraction patterns were taken in the range of $2^\circ \leq 2\theta \leq 70^\circ$ with a scan rate of $0.1^\circ 2\theta$ per minute.

B/Mg composite samples were prepared by placing bundles of boron fibers into titanium crucibles and infiltrating under pressure with molten magnesium according to a previously reported method [8]. The typical infiltration temperature and time was 800°C for 30 min. Select samples were heated at $950\text{-}1000^\circ\text{C}$ to facilitate further reaction between the boron fibers (doped and undoped) and the Mg matrix.

RESULTS

A series of SEM micrographs of boron fiber surfaces (Figure 2) shows fiber surface morphology as a function of carbon doping level. Undoped CVD B fibers appear amorphous by TEM. X-ray diffraction patterns (Figure 3a) are indicative of an amorphous phase. The “corn-cob” surface texture (insets to Figures 2a and 2b) is indicative of macroscopic growth morphology and not the size of individual grains. Below a carbon dopant level of 2%, the fiber surface morphology remained relatively unchanged and the boron phase remained x-ray amorphous. At the 2% dopant level, however (Figure 2c) there were isolated occurrences of much larger grains, $10\text{-}50\mu\text{m}$ in size, that were most likely seeded by a threshold concentration of carbon dopant. At the 3% dopant level (Figure 2d) rapid crystal growth dominates and the fiber no longer retained a regular cylindrical shape, but rather was a string of larger $10\text{-}50\mu\text{m}$ crystals irregularly arrayed around the tungsten boride substrate. X-ray diffraction of the 3% carbon-doped boron fiber indicates that it is well-crystallized tetragonal boron (Figure 3c). TEM was performed on fiber surfaces, broken shards of fibers, and samples prepared by ion beam thinning. High resolution TEM did not detect crystalline grains in the undoped B fibers. Tilting dark field imaging also did not exhibit significant crystallinity, indicating that the undoped B fibers are primarily amorphous, which is consistent with the above x-ray diffraction results. TEM observation of the crystallized fibers doped with 3% carbon showed grains $>10\text{-}20\mu\text{m}$ in size at the surface of the fiber. Selected area diffraction (SAD) showed that the fibers doped with high levels of carbon crystallized with the tetragonal phase of boron [10]. High resolution TEM images acquired at the [111] orientation were consistent with tetragonally crystallized boron formation in the 3% carbon-doped boron fiber. Quantitative EDS performed on spectra acquired from several thicknesses of crystallized B determined that carbon is present within the crystal and was not merely a surface contaminant during the analysis. Quantitative EDS also established that the carbon concentration is significantly less than 20 atomic %, thereby indicating the crystalline phase is not B_4C . Although over twenty B(low-C) phases are reported in the Powder Diffraction File (PDF) [11], the electron diffraction data of these crystallized fibers match best to results reported for pure tetragonal boron (PDF-74-0945). It is thus suggested that some of the many “pure” boron phases reported in the PDF may have some solubility for carbon.

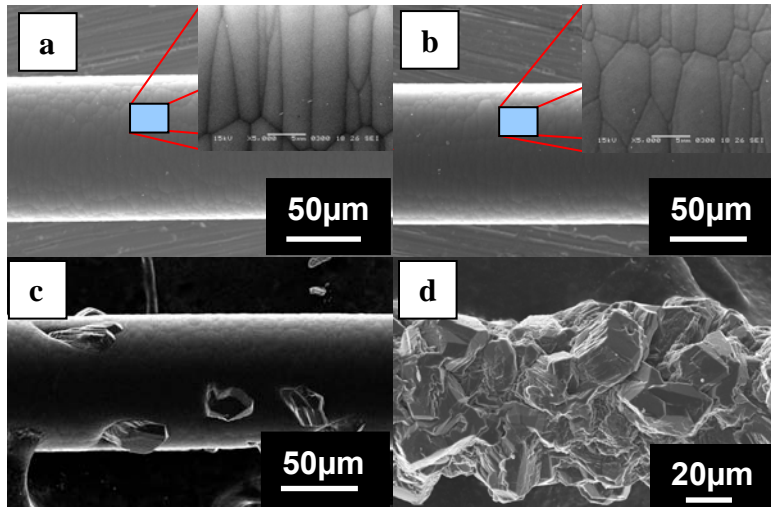


Figure 2. Surface morphology of boron fibers at the following carbon dopant levels in atomic percent: a) 0% b) 1.4% c) 2% and d) 3%. Insets to 2a and 2b show a 25µm wide area of the fiber surface.

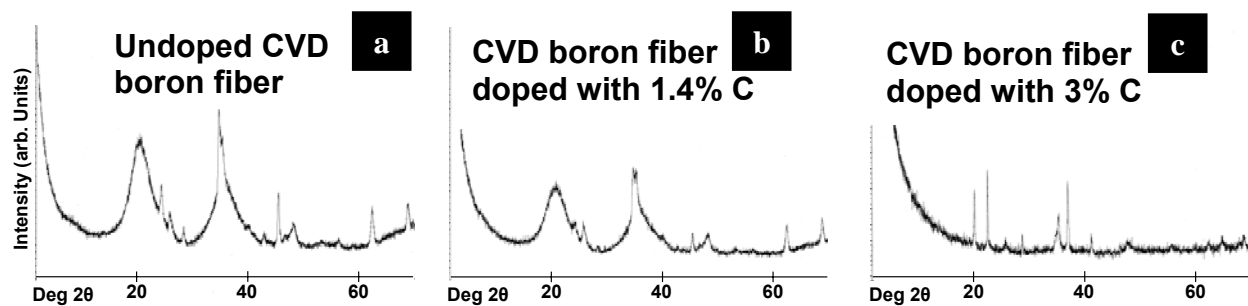


Figure 3. X-ray diffraction patterns of undoped and carbon-doped B fibers. Undoped boron and boron doped with 1.4% carbon consist of amorphous boron plus crystalline tungsten boride substrate material. Boron doped with 3% carbon is a well crystallized tetragonal boron phase.

TEM samples were prepared in cross section of the Mg-infiltrated B fibers, using polishing, dimpling and ion-beam thinning. The B fibers strongly resist thinning as compared to the surrounding matrix metal grains. Figure 4a is a bright field image of the interface between undoped B fiber and matrix in a composite infiltrated at 800°C. Four regions are visible: (i) the fiber interior (top region of 4a) is amorphous B; (ii) closer to the fiber-matrix interface is 0.5µm zone of fine grains (20-50nm); (iii) the fiber surface consists of a 1-2µm zone of coarser ~1µm grains; (iv) the bottom region in Figure 4a consists of the Mg matrix which was preferentially removed by TEM sample preparation. Figure 4b exhibits SAD of the fine-grain zone, with ring diffraction consistent with several B-Mg phases (such as MgB₄ or MgB₁₂). Figure 4c exhibits SAD of the next region with a [-1100] zone axis of the MgB₂ hexagonal phase. TEM analysis of the Mg matrix showed Mg metal grains >10-20µm in size extending across the entire matrix region between fibers. As infiltrated at 800°C, the reaction between B and Mg was limited to two thin layers indicated in Figure 4. Figure 5 shows optical micrographs of cross sections of composites that were heat treated at 1000°C (after the initial 800°C infiltration). A significant

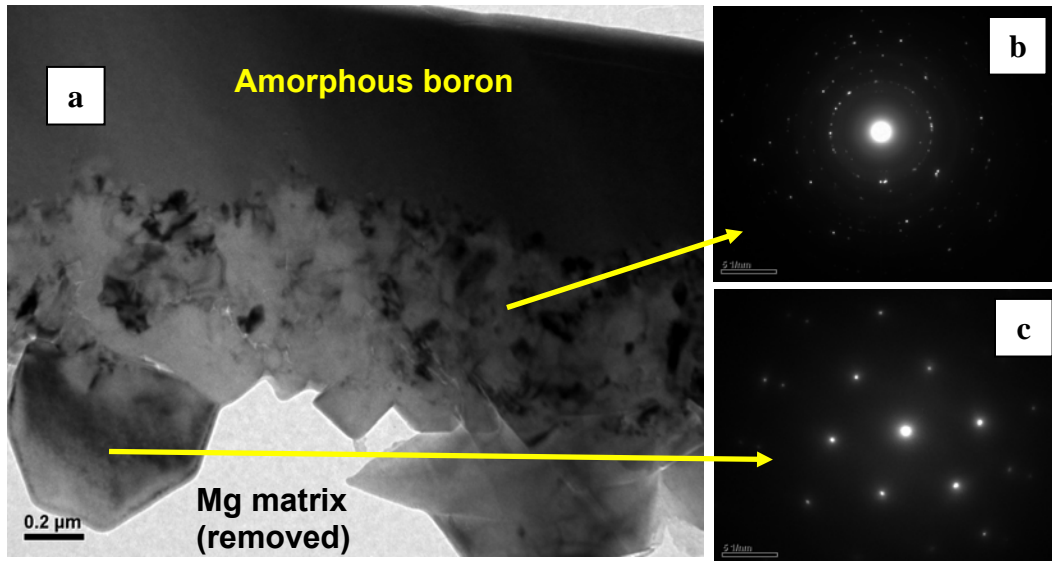


Figure 4. Bright-field TEM image (4a) at interface of undoped boron fiber and Mg matrix. 4b shows SAD of the finer-grained phase (SAD ring pattern consistent with MgB₄ or MgB₁₂), and EDS was consistent with a phase that is more boron-rich than the MgB₂ phase. 4c shows SAD indexed with the [-1100] zone orientation of the MgB₂ hexagonal phase.

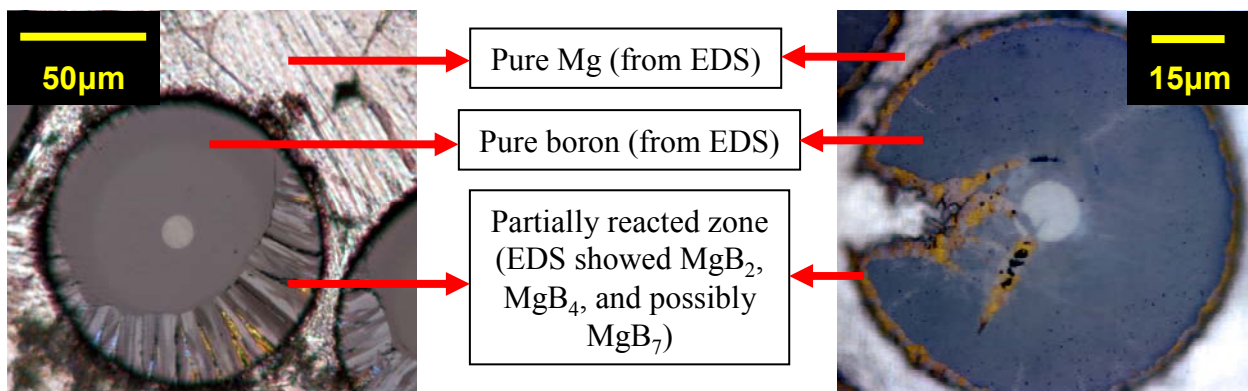


Figure 5. Polarized optical micrographs of composites made with undoped (left) and 0.5% C-doped (right) boron fibers. Undoped boron was heat treated at 1000°C for 15 min. C-doped boron (right) was heat treated at 1000°C for 16 hr. The Mg matrix partially reacted with the boron, although the C-doped boron fiber reacted much more slowly than the undoped fiber.

fraction of the undoped boron fibers reacted with the Mg after 15 min at 1000°C. The 0.5% C-doped boron fibers reacted much more slowly with the Mg matrix, exhibiting a reaction zone of <5 μm after more than 16 hr at 1000°C. The presence of carbon apparently inhibits the reaction between B and Mg, although the reason for this is not clear. The undoped and 0.5% C-doped boron fibers are both amorphous with similar crystallite sizes. Carbide phases at the C-doped fiber-matrix interface were not observed by TEM examination, although partial material loss

during sample preparation could explain this. SEM/EDS analysis of the partially reacted zones indicated a boron-rich composition suggesting that MgB_4 and/or MgB_7 form prior to complete reaction of the fiber to form MgB_2 . This is consistent with previous reports [3] in which boron fibers were reacted with Mg vapor. TEM analysis of Mg-B composites that were annealed at 950°C for 1 hour after the initial infiltration showed evidence of MgB_2 formation in the Mg matrix >100 μ m from the fiber-matrix interface.

CONCLUSIONS

The microstructure of boron fibers made by CVD was examined as a function of carbon dopant level. Undoped fibers and fibers doped with carbon at levels of <2 atomic % were found to be amorphous. At carbon dopant levels at $\geq 2\%$, the growth of large (10-50 μ m) grains of crystalline tetragonal boron was observed. It is suggested that there may be carbon present in the crystalline tetragonal phase of boron observed in fibers that were doped with higher concentrations ($\geq 2\%$) of carbon. Doped and undoped fibers were infiltrated with molten magnesium to form boron/magnesium metal matrix composites. At the 800°C infiltration temperature, a layer of MgB_2 was observed adjacent to the Mg matrix and a layer of boron-rich phase or phases (MgB_4 and/or higher borides) were observed adjacent to the boron fiber. Additional reaction at 950-1000°C resulted in further conversion of the fibers into a mixture of MgB_2 and higher borides (e.g. MgB_4), as well as increased formation of MgB_2 further into the Mg matrix. It was observed that C-doped boron fibers reacted with Mg much more slowly than undoped B fibers. Carbides were not observed at the fiber-matrix interface of the carbon-doped boron fibers reacted with Mg at 950-1000°C.

REFERENCES

1. R.J. Suplinskas and J.V. Marzik, "Boron and Silicon Carbide Filaments", in *Handbook of Reinforcements for Plastics*, edited by J.V. Milewski and H.S. Katz (New York: Van Nostrand Reinhold Co., 1987) pp. 340-363.
2. J. Nagamatsu, N. Nakagawa, T. Muranaka, Y. Zenitani, and J. Akimitsu, *Nature* **410**, 63 (2001).
3. P.C. Canfield, D.K. Finnemore, S.L. Bud'ko, J.E. Ostenson, G. Lapertot, C.E. Cunningham, and C. Petrovic, *Phys. Rev. Lett.* **86**, 2423, (2001).
4. D.K. Finnemore, W.E. Straszhiem, S.L. Bud'ko, P.C. Canfield, N.E. Anderson Jr., and R.J. Suplinskas, *Physica C*, **385**, 278 (2003).
5. N.E. Anderson Jr., W.E. Straszhiem, S.L. Bud'ko, P.C. Canfield, D.K. Finnemore, and R.J. Suplinskas, *Physica C*, **390**, 11 (2003).
6. R.H.T. Wilke, S.L. Bud'ko, P.C. Canfield, D.K. Finnemore, R.J. Suplinskas, and S.T. Hannahs, *Phys. Rev. Lett.* **92**, 217003 (2004).
7. R.H.T. Wilke, S.L. Bud'ko, P.C. Canfield, M.J. Kramer, Y.Q. Wu, D.K. Finnemore, R.J. Suplinskas, J.V. Marzik, S.T. Hannahs, "Superconductivity in MgB_2 doped with Ti and C", *Physica C*, in press (2004).
8. John D. DeFouw and David C. Dunand, *Appl. Phys. Lett.* **83**, 120 (2003).
9. P.C. Canfield and G.W. Crabtree, *Physics Today* **56**(3), 34 (2003).
10. J.L. Hoard, R.E. Hughes, D.E. Sands, *J. Am. Chem. Soc.* **80**, 4507 (1958).
11. International Center for Diffraction Data: Newtown Square, PA (2004).